*Transactions* of the SMiRT 27
Yokohama, Japan, March 3-8, 2024
Division XII

# Research Progress to Validate Applicability of Induction Bending for P91 Piping in Prototype Gen-IV Sodium-cooled Fast Reactor

**Tae-Won Na[1,2], Nak-Hyun Kim[3], Jong-Bum Kim[3], Chang-Gyu Park[3], Chang-Sung Seok[4] and Il-Kwon Oh[5]**

[1] Senior researcher, Korea Atomic Energy Research Institute (KAERI), Republic of Korea (ntw@kaeri.re.kr)
[2] PhD candidate, Korea Advanced Institute of Science and Technology (KAIST), Republic of Korea
[3] Principal researcher, Korea Atomic Energy Research Institute (KAERI), Republic of Korea
[4] Professor, Sungkyunkwan University, Republic of Korea
[5] Professor, Korea Advanced Institute of Science and Technology (KAIST), Republic of Korea

## ABSTRACT

The application of induction bending process for pipe fabrication in various industries is expanding. This is because the process can innovatively reduce the welded portion of the curved pipe, thereby reducing leakage due to cracks in the pipe welded portion. However, to date, there has been no case of applying induction bending to Gen-IV nuclear power plant piping operating in a high temperature environment.

In this study, we analyze the feasibility of applying induction bending fabrication to P91 bent pipe developed for Korea's PGSFR (Prototype Gen-IV Sodium-cooled Fast Reactor), from the perspectives of material fatigue properties and fatigue damage in pipe structures. Firstly, we conducted high-cycle and low-cycle fatigue tests on specimens taken from the bent pipe at a high-temperature environment (550°C). These tests verified that the pipes satisfy the design fatigue life criteria for P91 steel as stipulated in the ASME Boiler & Pressure Vessel Code, Section III, Division 5. Secondly, to efficiently determine test loads for structural testing of the pipes, a robust elastoplastic analysis model for the bent pipe was established, followed by detailed analyses. The specimen test results were used to ascertain the material constants for the Chaboche combined hardening model, which were then applied to the finite element analysis of the bent pipes to predict their behavior under both monotonic and cyclic loads. Third, a monotonic load test was performed on the bent pipe to analyze its behavior and compared with the elastoplastic analysis results to confirm the reliability of the analysis model. Furthermore, the design fatigue lives under cyclic loads were assessed by applying the ASME Code's inelastic analysis-based life assessment method, leading to the determination of effective fatigue test loads.

## INTRODUCTION

The Prototype Gen-IV Sodium-cooled Fast Reactor (PGSFR) is a Gen-IV sodium-cooled fast reactor developed in Korea as part of a national research and development project from 2012 to 2020. It is a 150MWe prototype reactor designed for demonstration purposes. The primary material for the high-temperature piping of the PGSFR, P91 (9Cr-1Mo-V), was chosen for its comparatively lower coefficient of thermal expansion compared to SS316, thus reducing thermal expansion and consequently reducing thermal stress in the piping. The high-temperature piping of the PGSFR includes many large-diameter, thin-walled curved pipes designed to reduce thermal stress. These numerous curved pipes are typically connected by welding, but welds are susceptible to leaks and can be a main cause of sodium leakage in sodium-cooled fast reactors. Therefore, as illustrated in Figure 1, applying the induction bending fabrication method, which manufactures straight pipe and curved pipe as an integral body, can significantly reduce the possibility of sodium leakage by minimizing the number of welds.

In this research, high-cycle and low-cycle fatigue tests at high temperature (550°C) were conducted on specimens from bent pipe under various force loads and strain range loads, respectively. These tests confirmed that the P91 bent pipes meet the design fatigue life criteria as specified in the ASME Boiler & Pressure Vessel Code, Section III, Division 5, thus validating the applicability of P91 bent pipes from the perspective of material fatigue properties. Also, the feasibility of using induction heating bent pipe structures is being reviewed through structural integrity tests under high-temperature fatigue loads. For this purpose, a reliable elastoplastic analysis model for induction heating fabricated P91 pipe was presented, and the analysis result was compared with the monotonic load test result with the bent pipe. Furthermore, the results of the elastoplastic analysis under cyclic loads were applied to the design fatigue curves of the ASME Code to determine the fatigue test loads effectively. Currently, fatigue testing on the bent pipe structures is underway.

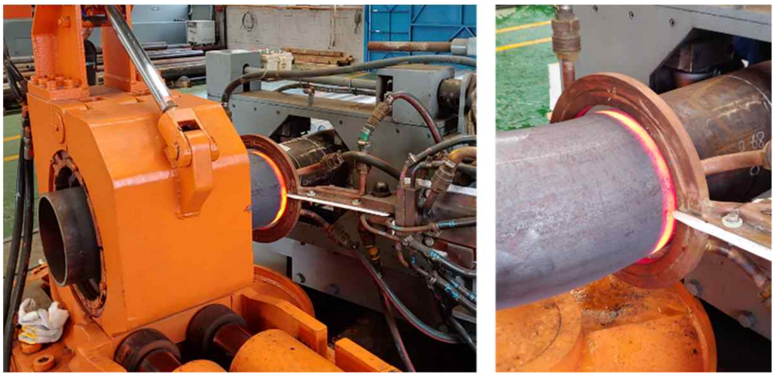

Figure 1. Fabrication of induction bent P91 pipe.

## VERIFICATION OF MATERIAL FATIGUE PROPERTY OF P91 BENT PIPE

### *Specimen Fabrication*

The P91 bent pipes fabricated using induction bending met all specified manufacturing requirements, and the nominal dimensions of the parent pipe were an outer diameter of 559 mm and a thickness of 12.7 mm. The radius of curvature of the bent pipe is 2DR, and the bending angle is 90˚. The shape of the fabricated pipe is illustrated in Figure 2(a). Based on the results of previous research on induction heating bent pipe material tests, which considered the average yield strength and tensile strength values of specimens from all sections, the extrados section was deemed representative. Therefore, the specimens for the high-temperature tensile tests and high-temperature fatigue tests in this study were fabricated from samples taken from the extrados section of elbow. The drawing of the test specimen is presented in Figure 2(b).

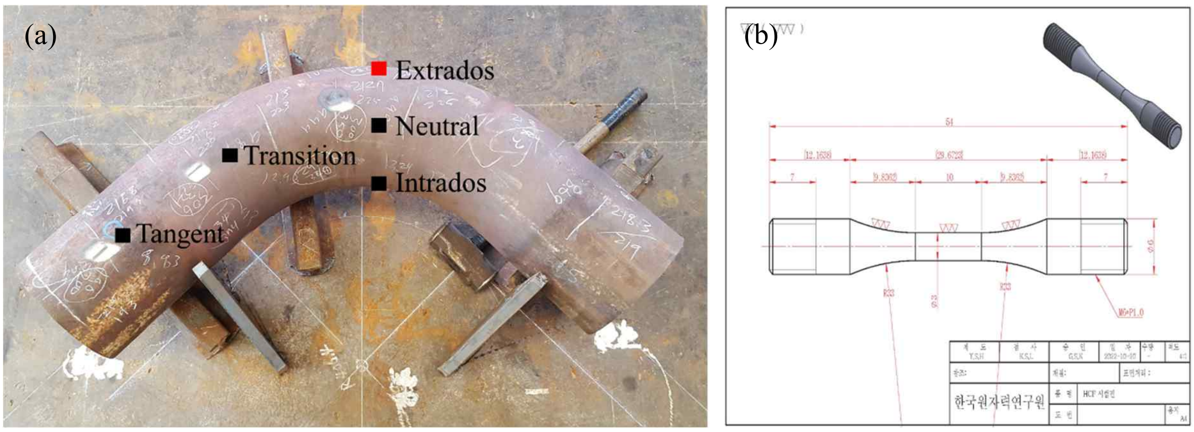


Figure 2. (a) P91 steel pipe fabricated by induction bending,
(b) drawing of the specimen test.

***Tensile Test***

The high-temperature tensile test was conducted at 550°C with a strain rate control of 0.001/sec. The result from the tensile test was used to determine the loading conditions for the high-cycle fatigue tests and low-cycle fatigue tests as shown in Figure 3. The elastic modulus, the proportional limit, yield strength (0.2% Offset), and tensile strength were measured as 174 GPa, 269 MPa, 337 MPa, and 461 MPa, respectively, with an elongation of 28%. The area (a) in Figure 3 was set as the high-cycle fatigue test load range (approximately 300 MPa to 430 MPa), and the area (b) was set as the low-cycle fatigue test load range (strain rate of 0.02 or more).

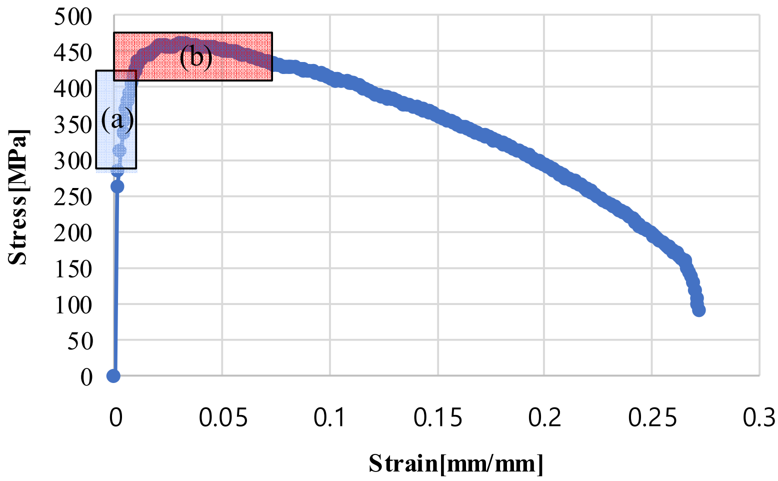


Figure 3. Tensile curve and load ranges for high-cycle and low-cycle fatigue tests.

***High-Cycle Fatigue Tests***

The high-cycle fatigue tests were conducted on nine specimens at 550°C, applying force loads from 260 kg to 320 kg as maximum loads. A load ratio (R) of 0.1 and a cyclic load frequency of 2 Hz were applied. To quantitatively assess the fatigue properties of P91 steel fabricated by induction bending, a comparison with the standard fatigue properties of typical P91 steel is necessary. Since the design fatigue curves presented in the ASME Code are based on a load ratio of -1, the stress results from tests conducted at a load ratio of 0.1 were converted to equivalent stresses at a load ratio of -1 using Goodman's diagram, and the results are presented in Table 1. Except for Specimen #1 and Specimen #2, which are the loads most affected by plasticity, the stress amplitude at -1 load ratio for the remaining specimens was converted to strain amplitude by dividing it by the elastic modulus.

***Low-Cycle Fatigue Tests***

The low-cycle fatigue tests were conducted at a temperature of 550°C with a strain rate of 0.002/sec and strain control at a load ratio of -1. A total of seven specimens were tested, each at different strain range values ranging from 0.02 mm/mm to 0.08 mm/mm. The low-cycle fatigue test results and the half cyclic curve, obtained using the stress ranges of the stabilized cycles for each load condition, are shown in Table 2 and Figure 4, respectively. In Figure 4, the half cyclic curve is positioned below the tensile curve, indicating lower stress. This is a typical characteristic of metal that exhibit cyclic softening behaviour, such as P91 steel, and it was confirmed that P91 bent pipe subjected to induction bending also undergoes cyclic softening.

Table 1: Results of high-cycle fatigue tests on specimens.

| Load ratio | 0.1 | | | | -1 | | | | - |
|---|---|---|---|---|---|---|---|---|---|
| - | Max. stress [MPa] | Min. stress [MPa] | Mean stress [MPa] | Stress amplitude [MPa] | Mean stress [MPa] | Stress amplitude [MPa] | Strain range [mm/mm] | Total strain range [mm/mm] | Cycles to failure [$N_f$] |
| Specimen | $\sigma_{max}$ | $\sigma_{min}$ | $\sigma_{mean}$ | $\sigma_a$ | $\sigma_{mean}$ | $\sigma_a$ | $\varepsilon_a$ | $\Delta\varepsilon$ | N |
| #1 | 444 | 44 | 244 | 200 | 0 | 425 | - | - | 25 |
| #2 | 430 | 43 | 237 | 194 | 0 | 398 | - | - | 1181 |
| #3 | 416 | 42 | 229 | 187 | 0 | 372 | 0.0021 | 0.0043 | 23,486 |
| #4 | 402 | 40 | 221 | 181 | 0 | 348 | 0.0020 | 0.0040 | 57,897 |
| #5 | 389 | 39 | 214 | 175 | 0 | 326 | 0.0019 | 0.0037 | 92,857 |
| #6 | 375 | 37 | 206 | 169 | 0 | 305 | 0.0018 | 0.0035 | 441,564 |
| #7 | 361 | 36 | 198 | 162 | 0 | 285 | 0.0016 | 0.0033 | over 1,000,000 |
| #8 | 423 | 42 | 233 | 190 | 0 | 385 | 0.0022 | 0.0044 | 18,392 |
| #9 | 389 | 39 | 214 | 175 | 0 | 326 | 0.0019 | 0.0037 | 198,642 |

Table 2: Results of low-cycle fatigue tests on specimens.

| Strain range (Total strain range) [mm/mm] | Cycles to failure [$N_f$] | Saturation cycles[N] | $\Delta\sigma/2$ [MPa] |
|---|---|---|---|
| ±0.02 (0.04) | 330 | 92 | 633 |
| ±0.03 (0.06) | 169 | 46 | 680 |
| ±0.04 (0.08) | 110 | 45 | 665 |
| ±0.05 (0.10) | 74 | 31 | 635 |
| ±0.06 (0.12) | 56 | 25 | 577 |
| ±0.07 (0.14) | 32 | 15 | 583 |
| ±0.08 (0.16) | 36 | 13 | 552 |

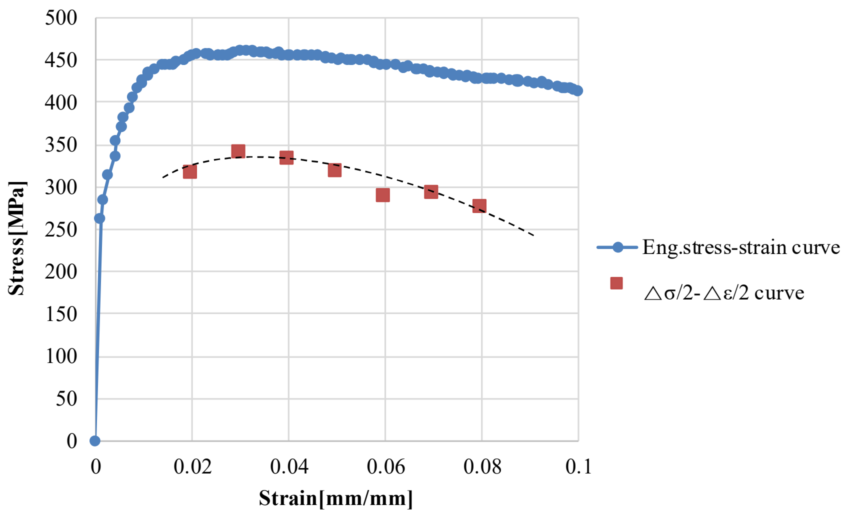


Figure 4. Comparison of the half cyclic curve of low-cycle fatigue tests with the tensile curve.

***Comparative Analysis of High-Cycle and Low-Cycle Fatigue Tests***

The results of high-cycle and low-cycle fatigue tests on the specimens were compared with design fatigue curve for P91 steel of the ASME Code. The design fatigue curve at 550°C was derived by linear interpolation of the curves provided for 540°C and 600°C in the creep-fatigue damage evaluation procedure of HBB-T-1400, of the ASME B&PV Code, Section III, Division 5. In addition, the fatigue test results and best fit fatigue life curve (the average test value fatigue curve), obtained by removing the margin of 2 for the strain rate range and 20 for the number of cycles conservatively applied to the design fatigue curve of the ASME Code, are compared in Figure 5. The data of the NIMS fatigue tests for the total strain range values between high-cycle and low-cycle fatigue tests in this study, were also added in Figure 5 for comparison with the best fit fatigue life curve, and they showed good agreements each other. In conclusion, it was verified that the curves obtained from the high-cycle and low-cycle fatigue tests of the induction bent P91 pipe material consistently showed similar trends to the best fit fatigue life curve of the typical P91 steel. The satisfactory compliance with the design fatigue properties required by the ASME Code, with significant margin, validates the applicability of induction bending for P91 pipes from the perspective of fatigue properties.

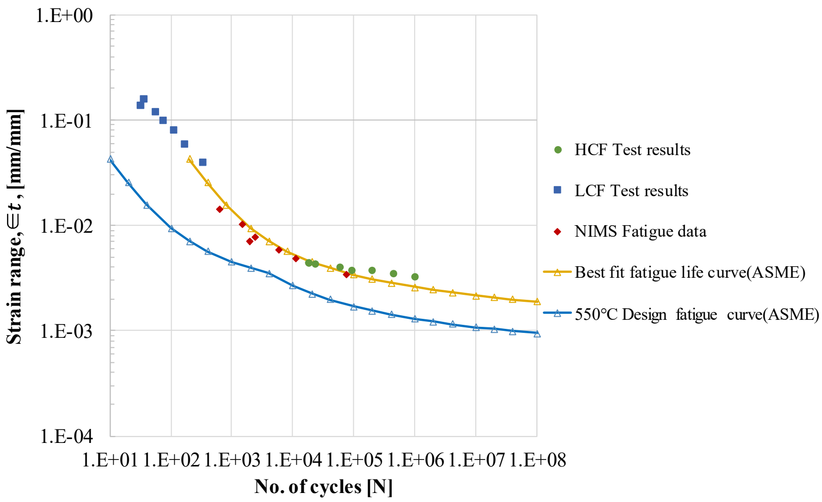


Figure 5. Comparison of high-cycle and low-cycle fatigue test results with the 550°C design fatigue curve (ASME) and the best fit fatigue life curve (ASME).

## Elastoplastic Analysis of Bent Pipe Structure

***Determination of Material Constants for the Chaboche Combined Hardening Model***

For an efficient structural test of bent pipe structures, it is necessary to first predict the inelastic behavior of induction heating bent pipe structures at high temperatures to appropriately set the test loads. For this purpose, it is necessary to develop a reliable elastoplastic analysis model for P91 pipes fabricated using induction bending, and to conduct analyses using this model. Therefore, it was decided to apply the Chaboche combined hardening model, which can simulate both kinematic hardening and isotropic hardening behaviors of P91 steel.

The yield function, for combined kinematic and isotropic hardening, depends on the stress, back stress ($X$) of the kinematic hardening, drag stress ($R$) of the isotropic hardening and yield stress ($\kappa$) as follows

$$f = |\sigma - X| - R - \kappa \tag{1}$$

$$\dot{X} = \frac{2}{3} C\, d\varepsilon^{p} - \gamma\, X\dot{p} \tag{2}$$

Where $C$ and $\gamma$ are two constants of kinematic hardening, $\gamma$ is the time constant which determines the rate of saturation of stress, and $C/\gamma$ is determines the magnitude of the back stress.

$$\dot{R} = b(Q - R)\dot{p} \tag{3}$$

Where $b$ and $Q$ are two constants of isotropic hardening, $Q$ is the asymptotic value which corresponds to regime of stabilized cycles, and $b$ indicates the speed of the stabilization.

The material constants for the elastoplastic analysis model, including those of the Chaboche combined hardening model determined using the results from the tensile tests and low-cycle fatigue tests of the specimens, are summarized in Table 3.

Table 3: Material constants for the elastoplastic analysis model of induction bent P91 pipe.

| Young's Modulus [GPa] | Poisson's Ratio | $\kappa$ [MPa] | $C$ | $\gamma$ | $Q$ | $b$ |
|---|---|---|---|---|---|---|
| 174 | 0.3 | 269 | 32,960 | 160 | -95 | 1.277 |

***Elastoplastic Analysis Model of Bent Pipe Structure***

The structural integrity test of the bent pipe structure at high temperature was conducted on an 8-inch diameter pipe of the PGSFR, and the drawing of the pipe to be tested is presented in Figure 6(a). The outer diameter of the pipe is 219.1 mm, and its thickness is 8.18 mm. The dimensions of the analysis model were determined by applying the actual measurements of the outer diameter and thickness at various locations of the P91 pipes, which were fabricated using induction bending. The shape and finite element model of the 1/2 bent pipe analysis model are shown in Figure 6(b), and 3D analysis was performed applying the Chaboche combined hardening model. For the finite element analysis, the commercial software ANSYS 2020R2 was used. The boundary conditions were set identical to the test conditions by fixing the displacement on the side of the flange at the bottom of the pipe structure. To simulate the application of the Y-axis directional load by the structural test rig on the pipe structure, a Y-axis directional displacement was applied to the hole shown in Figure 6(b) to perform monotonic and cyclic elastoplastic analyses.

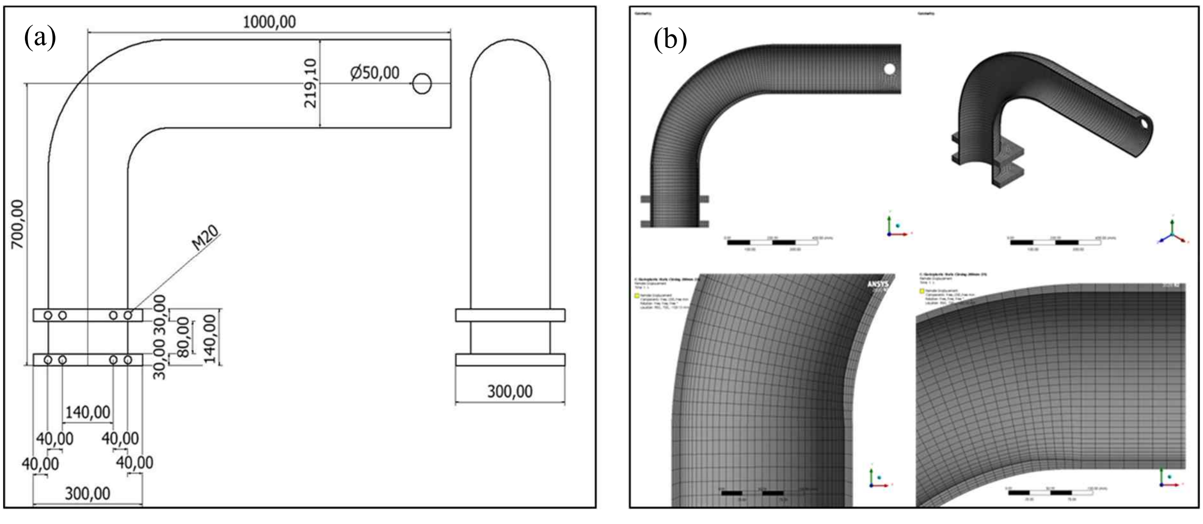


Figure 6. (a) Drawing of the bent pipe test structure (b) finite element model of the bent pipe.

### *Bent Pipe Elastoplastic Analysis for Monotonic Load Test*

The Y-axis reaction force to the Y-axis directional displacement load ranging from -200 mm to +200 mm at the load point was calculated, and the load-displacement curve is presented in Figure 7(a). Additionally, the stress distribution and the points of maximum stress occurrence for both opening and closing directional displacement loads are shown in Figure 8(a) and (b), respectively. It was observed that the maximum stress occurs on the inner surface of the neutral section of the bent pipe model.

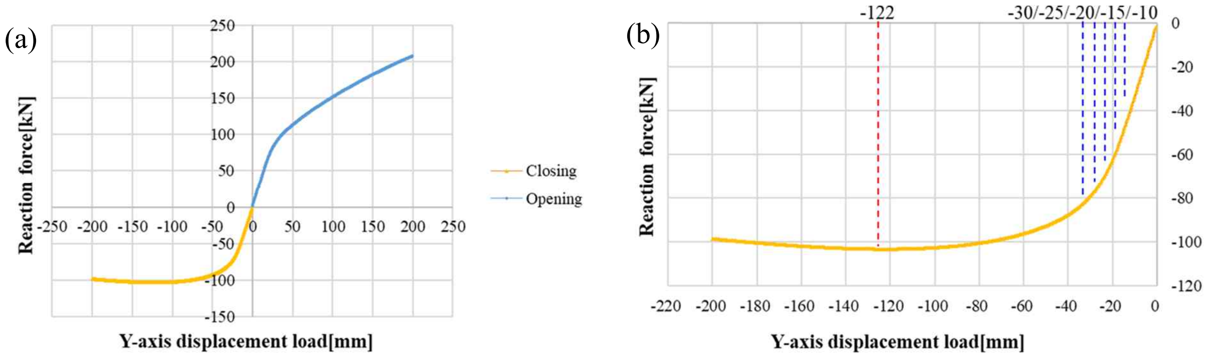


Figure 7. (a) Load-displacement result of monotonic load analysis, (b) load-displacement results of monotonic load in the closing direction and selection of fatigue test loads

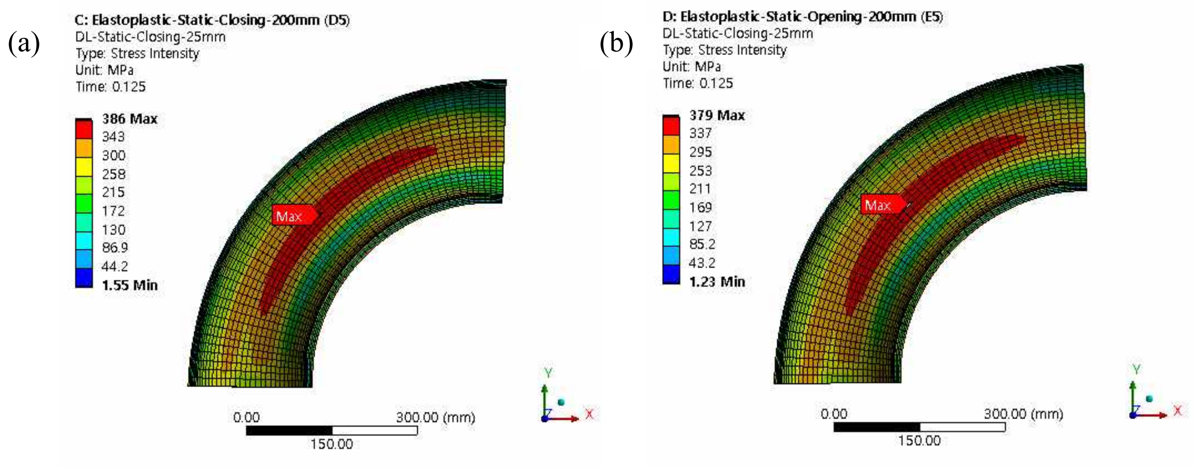


Figure 8. Stress distribution under (a) under closing directional load and (b) opening directional load.

### *Bent Pipe Elastoplastic Analysis for Cyclic Loads Tests*

Based on the Load-displacement result for monotonic load, it was decided to apply cyclic displacement loads smaller than the displacement load of 122mm, where the maximum reaction force occurs. Consequently, as indicated in Figure 7(b), Y-axis directional displacements with a load ratio of -1, specifically $\pm10$, $\pm15$, $\pm20$, $\pm25$ and $\pm30$ mm, were applied to the load point of the bent pipe analysis model. The load-displacement curves for one cycle with respect to displacement loads at the load point and the circumferential stress-strain analysis results at the point of maximum stress on the inner surface of the neutral section of the bent pipe model are as shown in Figure 9(a) and (b).

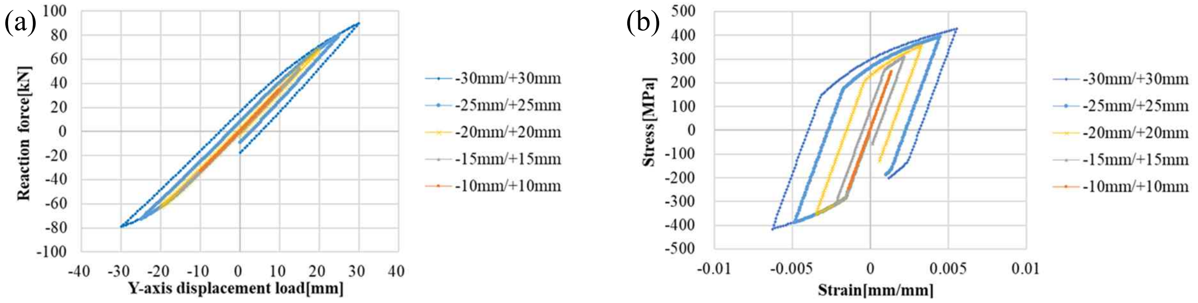


Figure 9. One cycle analysis result for each displacement load: (a) load-displacement at the load point, (b) circumferential stress-strain at max. stress point

## BENT PIPE STRUCTURAL INTEGRITY TEST

### *Monotonic Load Test of Bent Pipe Structure*

The monotonic load test of the bent pipe structure was conducted as shown in Figure 10(a), where the flange at the bottom of the structure was fixed to beams, and a load pin inserted into the hole of the pipe was used to apply vertical downward displacement load by an actuator, and the reaction force was measured. The drive part of the structural test rig is an Instron 8400 with a capacity of 25 tons, and as shown in Figure 10(b), an air circulation heater was installed inside the bent pipe to maintain the temperature of the bent section at 550°C(within ±2%) during test.

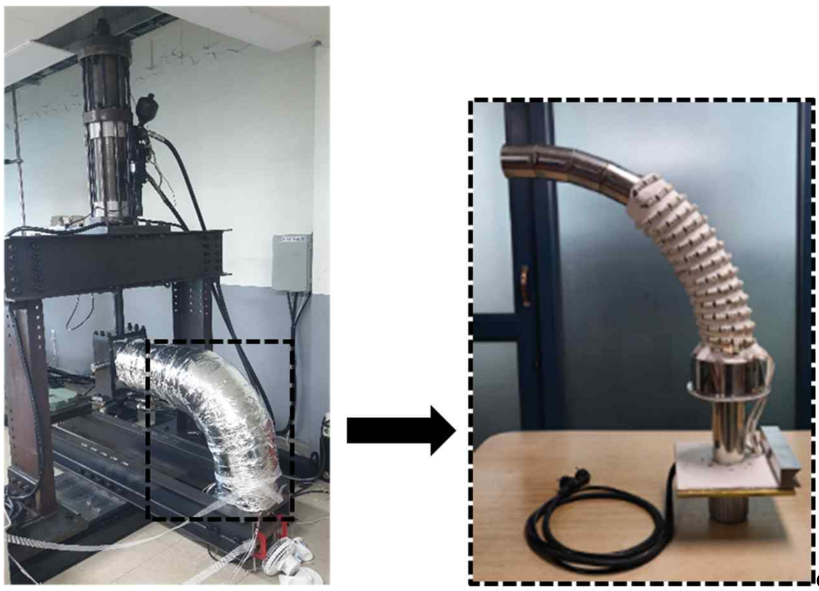

Figure 10. (a) Structural test rig for bent pipe structure, (b) internal air circulation heater.

The monotonic load test was conducted by applying a displacement load up to 65 mm, and the reaction force for this displacement load is shown in Figure 11. The results of the elastoplastic analysis of the bent pipe under monotonic load, previously introduced, were compared with the test results and presented in Figure 11. The maximum difference between the analysis and test results was 8%, which is deemed very satisfactory. Additionally, after the monotonic load test, the outer diameter of the plastically deformed pipe in the unloaded state was measured and compared with the analysis result under the same conditions. The maximum ovality of the pipe in both the test and analysis result was confirmed to be within 11.5% and 9.5%, respectively. Therefore, the elastoplastic analysis result for the bent pipe not only matched the Load-displacement results for monotonic load test but also the behavioral analysis results, thus verifying the reliability of the analysis model established in this study.

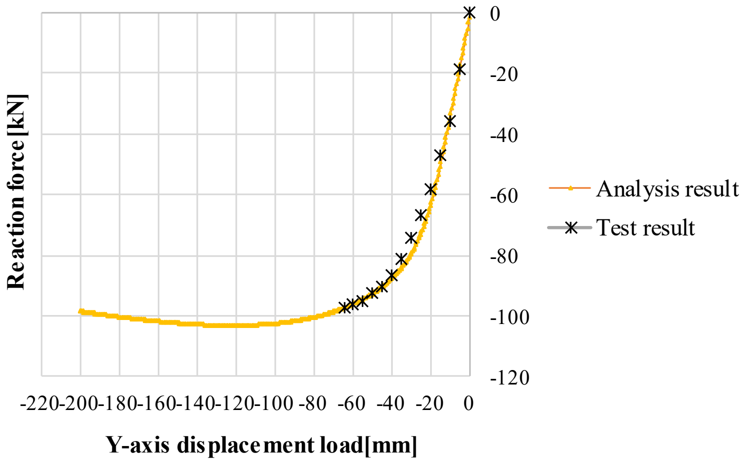


Figure 11. Comparison of Load-displacement for Monotonic Load of Bent Pipe Structure

***Determination of fatigue test load for bent piping structures***

Following the monotonic load analysis, cyclic load analysis of the bent pipe was conducted with respect to the selected displacement loads. The total strain range at the maximum stress point was calculated using the inelastic analysis method HBB-T-1420 of the ASME B&PV Code, Sec. III, Div. 5, for each load. Furthermore, as shown in Figure 12, the design fatigue life for the total strain range at 550°C for P91 steel according to the ASME Code was determined and summarized in Table 4. This plan is to verify structural integrity by performing fatigue tests with a margin added to the fatigue life for each load case in the Table 4. Currently, high-cycle fatigue tests are being conducted for the cyclic force loads equivalent to ±10, ±15 mm of displacement load respectively, and after these tests, fatigue damage inspection will be carried out using non-destructive inspections such as PT, MT and UT.

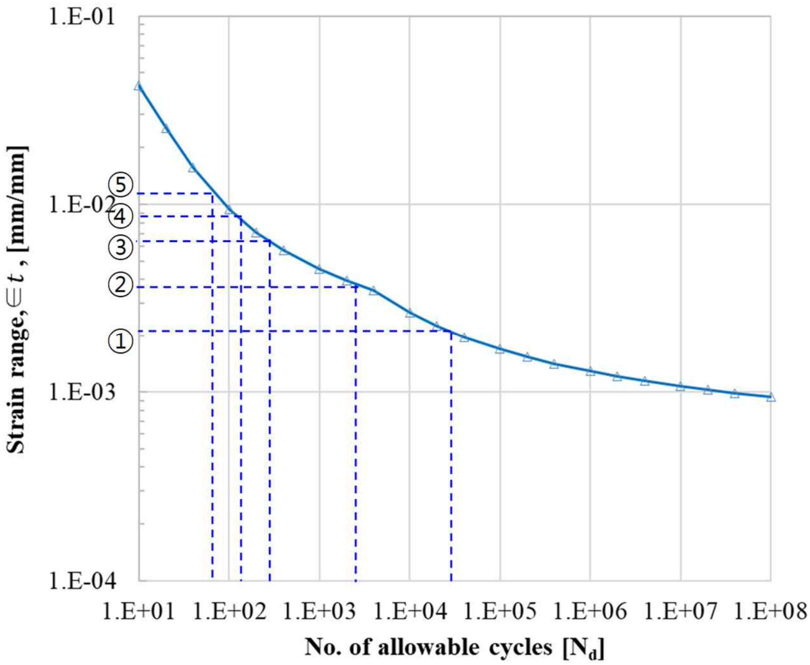


Figure 12. Design fatigue curve of 550°C for P91 steel in ASME Code and design fatigue life for cyclic displacement loads on the P91 bent pipe.

Table 4. Selection of fatigue test load for the P91 bent pipe.

| No. | Disp. Load [mm] | Total strain range [mm/mm] | Allowable cycles* [$N_d$] |
|---|---|---|---|
| ① | Δ±10 | 2.32E-03 | 17,742 |
| ② | Δ±15 | 3.88E-03 | 2,174 |
| ③ | Δ±20 | 6.22E-03 | 302 |
| ④ | Δ±25 | 8.76E-03 | 120 |
| ⑤ | Δ±30 | 1.13E-02 | 73 |

* Allowable cycles of 550°C design fatigue curve for P91 in from ASME Code

## CONCLUSION

Structural integrity of P91 induction bent pipe was evaluated through high-temperature fatigue tests on material specimens extracted from the pipe and on the bent pipe structure itself. To achieve this, high-temperature fatigue tests on the specimens under various loads were performed, confirming that they satisfied the design fatigue life criteria sufficiently specified in ASME Code. Additionally, the fatigue test results were found to be close to the best fit fatigue life curve from the ASME Code. An elastoplastic analysis model incorporating the Chaboche combined hardening model for induction bent P91 pipe was developed and applied to perform elastoplastic analyses under monotonic and cyclic loads. The reliability of the analysis model was confirmed by comparing the monotonic load test result of the bent pipe structure with the analysis result, and appropriate fatigue test loads for the pipe structures were determined using the analysis results for the cyclic loads and the ASME Code design fatigue curve. Using the loads determined through this process, fatigue tests on the bent pipe are undergoing, and following the tests, fatigue damage inspection using non-destructive inspection will be carried out to evaluate the structural integrity of the pipe structure. Furthermore, after validating the applicability of P91 induction bent pipes under fatigue loads, we plan to verify structural integrity further against creep and creep-fatigue loads in the near future.

## ACKNOWLEDGMENTS

This work was supported by a grant from the National Research Foundation of Korea (NRF) funded by the Korean government (Ministry of Science and ICT) (NRF-2021M2E2A1037872).

## REFERENCES

Yoo, J. W., Chang, J. W., Lim, J. Y., Cheon, J. S., Lee, T. H., Kim, S. K., Lee, K. L. and Joo, H. K. (2016). “Overall system description and safety characteristics of prototype Gen IV sodium cooled fast reactor in Korea,” Nuclear Engineering and Technology, Korea, 48(5), 1059-1070.
ASME International. (2021). ASME Boiler and Pressure Vessel Code. USA.
ASME. (2007). ASME B31.1, Power Piping Code. USA.
Pipe Fabrication Institute. (2010). PFI standard ES-24, Pipe Bending Methods, Tolerances, Process and Material Requirements, USA and Canada.
Kim, N. H., Kim, J. B. and Kim, S.K. (2021). “Applicability of the induction bending process to the P91 pipe of the PGSFR,” Nuclear Engineering and Technology, Korea, 53(5), 1580-1586.
NRIM. (1993). NRIM fatigue data sheet, No.78, Data sheets on elevated-temperature, time-dependent low-cycle fatigue properties of ASTM A387 Grade 91 steel plate for pressure vessels. Japan.
Chaboche, J. L. (1990). Mechanics of Solid Materials., Cambridge University Press.
Ansys 2020 R2. (2020).